Published Ahead of Print on June 16, 2020 as 10.1212/WNL.0000000000010116

Neurology®
The most widely read and highly cited peer-reviewed neurology journal
The Official Journal of the American Academy of Neurology

AMERICAN ACADEMY OF NEUROLOGY®

**Neurology Publish Ahead of Print**
**DOI: 10.1212/WNL.0000000000010116**

# Early postmortem brain MRI findings in COVID-19 non-survivors

*Tim Coolen, MD[1,2*]; Valentina Lolli, MD[1,2*]; Niloufar Sadeghi, MD, PhD[1]; Antonin Rovaï, PhD[2,3]; Nicola Trotta, PhD[2,3]; Fabio Silvio Taccone, MD, PhD[4]; Jacques Creteur, MD, PhD[4]; Sophie Henrard, MD[5]; Jean-Christophe Goffard, MD, PhD[5]; Olivier De Witte, MD, PhD[6]; Gilles Naeije, MD, PhD[3,7]; Serge Goldman, MD, PhD[2,3]; Xavier De Tiège, MD, PhD[2,3]*

[1]Department of Radiology, CUB Hôpital Erasme, Université libre de Bruxelles (ULB), Brussels, Belgium.

[2]Laboratoire de Cartographie fonctionnelle du Cerveau, UNI — ULB Neuroscience Institute, Université libre de Bruxelles (ULB), Brussels, Belgium.

[3]Department of Nuclear Medicine, CUB Hôpital Erasme, Université libre de Bruxelles (ULB), Brussels, Belgium.

[4]Intensive Care Unit, [5]Department of Internal Medicine, [6]Department of Neurosurgery, and [7]Department of Neurology, CUB Hôpital Erasme, Université libre de Bruxelles (ULB), Brussels, Belgium.

*These authors contributed equally to the study

**Corresponding Author:** Xavier De Tiège, xdetiege@ulb.ac.be

**Words count:** 4494, **Abstract**: 220 words, **Character count of the title:** 54

**Figures:** 6, **Tables:** 1

**Supplemental Data (https://doi.org/10.5061/dryad.4qrfj6q7p):** 3 e-Tables, 1 e-Figure.

[ 142 ] Viral infections, [ 146 ] All Medical/Systemic disease, [ 7 ] Intracerebral hemorrhage, [ 13 ] Other cerebrovascular disease/ Stroke, [ 120 ] MRI

*Publication History :* A preprint of this Article (without the supplementary material) has been uploaded to the MedRxiv server (https://medrxiv.org/cgi/content/short/2020.05.04.20090316v1).

*Study Funding :* This work was supported by a special call “COVID-19” funded by the Université libre de Bruxelles, the Fonds Erasme (Brussels, Belgium) and the Fondation ULB

(Brussels, Belgium). The PET-MR project at the CUB Hôpital Erasme and Université libre de Bruxelles is financially supported by the Association Vinçotte Nuclear (AVN, Brussels, Belgium). Tim Coolen is Clinical Master Specialist applicant to a PhD at the Fonds de la Recherche Scientifique (FRS-FNRS, Brussels, Belgium). Gilles Naeije and Xavier De Tiège are Postdoctorate Clinical Master Specialists at the FRS-FNRS (Brussels, Belgium).

*Role of the Funder/Sponsor:* The funding sources had no role in the design and conduct of the study (collection, management, analysis, and interpretation of data); in the preparation, review and approval of the manuscript; and decision to submit the manuscript for publication.

*Conflict of interest disclosure:* The authors report no disclosures relevant to the manuscript.

**Abstract**

*Objectives:* The severe acute respiratory syndrome coronavirus 2 (SARS-CoV-2) is considered to have potential neuro-invasiveness that might lead to acute brain disorders or contribute to respiratory distress in patients with coronavirus disease 2019 (COVID-19). This study investigates the occurrence of structural brain abnormalities in non-survivors of COVID-19 in a virtopsy framework.

*Methods:* In this prospective, monocentric, case series study, consecutive patients who fulfilled the following inclusion criteria benefited from an early postmortem structural brain MRI: death <24 hours, SARS-CoV-2 detection on nasopharyngeal swab specimen, chest computerized tomographic (CT) scan suggestive of COVID-19, absence of known focal brain lesion, and MRI compatibility.

*Results*: Among the 62 patients who died from COVID-19 from 31/03/2020 to 24/04/2020 at our institution, 19 decedents fulfilled the inclusion criteria. Parenchymal brain abnormalities were observed in 4 decedents: subcortical micro- and macro-bleeds (2 decedents), cortico-subcortical edematous changes evocative of posterior reversible encephalopathy syndrome (PRES, one decedent), and nonspecific deep white matter changes (one decedent). Asymmetric olfactory bulbs were found in 4 other decedents without downstream olfactory tract abnormalities. No brainstem MRI signal abnormality was observed.

*Conclusions*: Postmortem brain MRI demonstrates hemorrhagic and PRES-related brain lesions in non-survivors of COVID-19. SARS-CoV-2-related olfactory impairment seems to be limited to olfactory bulbs. Brainstem MRI findings do not support a brain-related contribution to respiratory distress in COVID-19.

## Introduction

Infection by the severe acute respiratory syndrome coronavirus 2 (SARS-CoV-2), named coronavirus disease 19 (COVID-19) by the World Health Organization, is associated with an ongoing worldwide outbreak of atypical and severe pneumonia.[1,2]

SARS-CoV-2 uses human cell receptor angiotensin-converting enzyme 2 (ACE2) as cellular entry point.[3] ACE2 is expressed in airway epithelia, lung parenchyma, vascular endothelium, heart, kidneys, and small intestine,[4] which explains most of COVID-19 symptoms. ACE2 is also present in glial cells and neurons of mammalian brain, especially in brainstem nuclei involved in cardio-respiratory function.[4] SARS-CoV-2 is therefore considered to have potential neuro-invasiveness that might lead to acute brain disorders or contribute to respiratory distress in COVID-19 patients.[5,6] SARS-CoV-2 might enter the central nervous system (CNS) through hematogenous dissemination or neuronal retrograde route via, e.g., olfactory bulbs or medullary neurons.[6] The anosmia frequently observed in SARS-CoV-2 infected patients[7,8] supports the neural retrograde hypothesis. The neuro-invasiveness of SARS-CoV-2 is also supported by case reports of meningo-encephalitis,[9–11] intracerebral hemorrhage,[12] ischemic strokes,[13] and secondary acute necrotizing encephalopathy[14] associated with SARS-CoV-2 infection. Central neurological symptoms (e.g., headache, stroke, impaired consciousness) are also observed in 25% of COVID-19 patients.[15] Still, brain magnetic resonance imaging (MRI) data are scarce in COVID-19 patients due to difficulties to obtain such examination in infected unstable patients during the COVID-19 outbreak.[15]

This prospective, monocentric, postmortem brain MRI case series investigated the occurrence of structural brain abnormalities in non-survivors of COVID-19 in a brain virtopsy framework performed early (≤24h)

after death. We specifically searched for signs of acute brain injury (e.g., stroke, encephalitis) and MRI signal abnormalities along the olfactory tract and brainstem.

## Methods

### *Study Design and participants*

From 31/03/2020 to 24/04/2020, consecutive decedents who fulfilled the following inclusion criteria were included: death <24 hours; SARS-CoV-2 detection (direct antigen detection or reverse transcriptase polymerase chain reaction (rtPCR)) on nasopharyngeal swab specimen, chest computerized tomographic (CT) scan suggestive of COVID-19 without alternative diagnosis; absence of known focal brain lesion; MRI compatibility. Clinical data were retrieved from decedents' medical record and reviewed by clinicians (F.S.T., S.H., J.C.G., G.N., O.D.).

After death, decedents were directly placed in an MRI-compatible mortuary bag, brought to the morgue, and placed in dedicated mortuary refrigerators (2-3 C°).

### *Standard Protocol Approvals, Registrations, and Patient Consents*

This study was carried out at the CUB Hôpital Erasme (Brussels, Belgium) after approval by the institutional Ethics Committee (Ref: P2020/204, SRB2020121), which did not request informed consent from legal representatives.

### *Clinical definitions*

Bilateral chest infiltrates associated with a $Pa0_2/FiO_2$<300 in ambient oxygen conditions or oxygen saturation < 90% during administration of at least 50% oxygen fraction

($FiO_2$) were identified as severe respiratory failure. Acute kidney injury was defined according to the Kidney Disease Improving Global Outcomes criteria.[16] Hypoxic hepatitis was defined as an increase in aspartate (AST) and/or alanine transaminases (ALT) more than 20 times the upper normal range (≤50 IU/L), i.e. >1,000 IU/L in the setting of acute cardiovascular failure and in the absence of another cause of cell necrosis.[17] Disseminated intravascular coagulation was defined according to standard criteria.[18] Acute cardiac injury associated with COVID-19 was identified according to recently proposed definitions.[19]

***MRI data acquisition***

Postmortem structural brain MRI were performed on a 3 Tesla hybrid PET-MR scanner (SIGNA™, GE Healthcare) in accordance with COVID-19 institutional hygienic and safety rules. During the COVID-19 outbreak, the PET-MR facility was isolated from the rest of the Nuclear Medicine Department, and dedicated to research investigations on COVID-19. This avoided any interference with ongoing clinical activities of the Department. Mortuary bags were not opened during the procedure.

MRI sequences consisted of whole-brain axial 3D T1-weighted imaging (WI, repetition time (TR)/echo time (TE)/Flip Angle (FA): 8ms/3ms/12°, inversion time (TI): 450ms, field of view (FOV): 24cm x 24cm, matrix: 240 x 240, resolution: 1mm x 1mm x 1mm), axial T2WI (TR/TE/FA: 6500ms/126ms/142°, FOV: 24cm x 24cm, matrix: 480 x 480, resolution: 0.5mm x 0.5mm x 3mm, slice spacing: 0.3mm), sagittal 3D T2WI FLAIR (TR/TE/FA: 7200ms/120ms/90°, TI: 1333 to 2041 ms, FOV: 25.6cm x 25.6cm, matrix: 256 x 256, resolution 1mm x 1mm x 1.4mm), axial 3D SWI (TR/TE/FA: 48ms/25ms/10°, FOV:

24cm x 24cm, matrix: 240 x 240, resolution: 1mm x 1mm x 1.6mm), and axial DWI (TR/TE/FA: 6500ms/80ms/90°, FOV: 26cm x 26cm, matrix: 128 x 128, resolution: 2mm x 2mm x 4mm, slice spacing: 0.4mm). The TI of the 3D T2WI FLAIR sequence was adapted for each patient as this parameter strongly depends on the decedents' body temperature,[19,20] which was dependent on the time spent by decedents in mortuary refrigerators. In our case, TI was adapted in a trial-and-error fashion to minimize the CSF signal, except for D1. A coronal T2WI (TR/TE/FA: 6500ms/112ms/142°, FOV: 15cm x 15cm, matrix: 256 x 256, resolution: 0.6mm x 0.6mm x 3mm, slice spacing: 0.2mm) centered on olfactory bulbs completed the acquisition. Total acquisition time was about 40 min.

***MRI data analyses***

MRI data were first independently reviewed by three neuroradiologists (V.L., T.C., N.S.) based on systematic and comprehensive visual assessment. Final reports were then discussed with three neurologists (S.G., X.D.T., G.N.) and with other clinicians (F.S.T., S.H., J.C.G., O.D.).

*Brain MRI findings reflecting postmortem changes*

MRI data were first screened for signal abnormalities that could be confidently attributed to early postmortem changes according to the existing literature.[21–24] Reported findings include increased T1WI signal of basal ganglia and thalami, suppression of fat signal intensity on T2WI, increased signal intensity of the cortical ribbon and the ventricular wall on DWI, and globally reduced apparent diffusion coefficient (ADC) values in the brain parenchyma. MRI data were also screened for potential additional postmortem changes, which, to the best of our knowledge, have not been reported. The increase in T1WI signal intensity was classified as absent (0), mild (1), or marked (2). The suppression of fat on

T2WI was categorized as incomplete (1) or complete (2). The cortical and periventricular rim-like increased signal intensity on DWI was also classified as incomplete (1) or complete (2). ADC values were measured by using three ellipsoid regions of interest (ROIs) in the left centrum semiovale, left thalamus/lenticular/caudate nuclei and left cerebellum.

Assuming that most postmortem MRI signal changes were related to changes in body temperature and therefore changes in T1 and T2 relaxation times of tissues, we postulated that signal abnormalities might increase with the delay between death and MRI data acquisition. We therefore performed Spearman's rank correlation between scan delay and adjusted FLAIR TI needed for adequate water suppression (excluding D1), T1 increased signal intensity, T2WI fat suppression and DWI increased signal intensity scores as well as the sum of ADC values. Correlation results were considered significant for $p<.05$ corrected for multiple comparisons.

*Brain MRI findings reflecting antemortem changes*

MRI data were subsequently screened for signal abnormalities reflecting antemortem changes. These were distinguished into recent (i.e., potentially related to COVID-19) and long-standing (i.e., unlikely related to COVID-19) changes. Recent changes included hemorrhages, oedema, and olfactory clefts and bulbs abnormalities. Hemorrhages were considered recent if hyperintense on T1WI or in the absence of signal abnormality suggestive of cerebral amyloid angiopathy or small vessel disease.[25] Long-standing signal abnormalities included white matter changes with an imaging pattern suggestive of microvascular ischemic chronic disease, enlargement of perivascular spaces, cerebral atrophy, and late-stage lacunar ischemic or hemorrhagic changes. The severity of T2/FLAIR white matter hyperintensities of presumed vascular origin was coded according to the Fazekas scale from 0 to 3 on T2WI and T2WI FLAIR sequences.[26] Basal ganglia and centrum semiovale enlargement of perivascular

spaces was rated with a total score ranging from 0 to 8 on axial T2WI sequences.[27,28] Cerebral atrophy was assessed by using both the simplified global cortical atrophy score,[29] retaining the worst (highest) score across the brain, and by calculating Evan's index[30] on 3D T1WI sequences. Supra- and infratentorial cortical sequelae and deep lacunes, pontine micro-ischemic leukoencephalopathy as well as presumed old micro- or macro-hemorrhages were also noted.

***Data availability***

De-identified postmortem brain MRI data can be shared upon reasonable request for scientific purpose and after approval of the CUB Hôpital Erasme Ethics Committee and authorities.

**Results**

Table 1 summarizes included decedents' characteristics.

Clinical and biological data of included decedents are detailed in Table e-1 available from Dryad: https://doi.org/10.5061/dryad.4qrfj6q7p.

Among the 62 patients who died from COVID-19 infection during the inclusion period, 19 decedents fulfilled inclusion criteria. The time interval between death and MRI acquisition varied between 2.07 and 23.75 hours (mean: 13.67 hours). Forty-three decedents were excluded from this study because of an excessive delay (>24h) between death and first MRI scanning opportunity (n=18), negative rtPCR on nasopharyngeal swab specimen (n=7), negative chest CT-scan findings (n=6), history of focal brain lesion (n=10), MRI incompatibility (n=2).

The mean age of included decedents was 77 (range: 49-94) years. All decedents had severe COVID-19 with 1 up to 5 comorbidities (i.e., hypertension, cardiac disorder, diabetes, chronic obstructive pulmonary disorder, chronic kidney disease, or body mass index >25). Anosmia was not reported in any decedent, but it was not systematically assessed. Decedents developed typical COVID-19 complications such as coagulopathy (6/19), acute kidney injury (14/19) or acute cardiac injury (18/19). D-dimer level was abnormal in all tested decedents (11/19). The assessment of arterial hypertension before death was limited for most patients admitted to COVID-19 wards due to their respiratory distress and end-of-life status. Among the patients who died at the intensive care unit (ICU; decedent 2 (D2), D8, D9, D15, D19), none had mean arterial pressure >100 mmHg and most of them received vasopressors before death to achieve at least 65 mmHg of mean arterial pressure. Mechanical ventilation was used in the five decedents hospitalized at the ICU, and two of them (D2 and D9) were placed on veno-venous extracorporeal membrane oxygenation (ECMO). None of the 14 decedents hospitalized in COVID-19 wards benefited from mechanical ventilation. Fifteen decedents died from respiratory failure, while 4 died from septic shock and multiorgan failure. All decedents were on anticoagulation (therapeutic, 6/19; prophylactic, 13/19).

*Brain MRI findings reflecting postmortem changes*

Signal abnormalities consistent with early post-mortem changes are detailed in Table e-2 available from Dryad: https://doi.org/10.5061/dryad.4qrfj6q7p.

The increase in T1WI signal intensity, when present, did not involve homogeneously the basal ganglia and the thalami but was limited to pallidi and postero-lateral thalami (Figure 1). Moreover, a similar increase in T1WI signal intensity was also present in the substantia nigra (SN), red nuclei (RN), and dentate nuclei (DN) in many decedents (Figure 1). These gray matter structures were thus included in the analysis of postmortem T1WI signal intensity

changes in addition to pallidal nuclei and postero-lateral thalami. The only decedent (D11) who did not show clearly increased T1WI signal intensity in any of the abovementioned deep nuclei was scanned after a delay of 3.38 hours, while decedents who had increased signal intensity in all these structures (D2, D8, D9, D10, D12, D16-19) had a scan delay ranging from 14.90 hours (D12) to 23.75 hours (D16).

—Place Figure 1 about here—

Suppression of fat on T2 WI was observed in all decedents. It was classified as complete (2) in 13/19 (mean scan delay: 17.74 hours, range: 4.35 - 23.75 hours) and incomplete (1) in 6/19 (4.85 hours, 2.07 - 12.28 hours) decedents (Figure 2). There was in all cases some degree of marked subcutaneous fat suppression but not systematically in the deep orbital fat (Figure 2).

On DWI, a cortical and periventricular high signal intensity rim was present in all decedents. It was classified as complete (2) in 15/19 decedents (mean scan delay: 16.38 hours, range: 2.80 - 23.75 hours) and incomplete (1) in 4/19 (3.51 hours, 2.07 - 5.05 hours; Figure 3). A clear correspondence with ADC map or other sequences data was not found.

All decedents presented a diffuse reduction of ADC across the brain parenchyma. ADC values ranged from 152 $x10^{-6}$ $mm^2/s$ (D10 and D17; scan delays of 18.75 and 21 hours respectively) to 347 $x10^{-6}$ $mm^2/s$ (D15; scan delay of 4.35 hours) in left centrum semiovale; 216 $x10^{-6}$ $mm^2/s$ (D10; 18.75 hours) to 503 $x10^{-6}$ $mm^2/s$ (D11; 3.38 hours) in left basal ganglia/thalamus; 152 $x10^{-6}$ $mm^2/s$ (D17; 21 hours) to 434 $x10^{-6}$ $mm^2/s$ (D15; 4.35 hours) in left cerebellum.

All decedents exhibited vascular signal loss on SWI images, some of them with increased visibility of vessels. The increased visibility of vessels was categorized as absent (0), discrete (1), moderate (2), or marked (3) on axial minimum intensity projections (10 mm thickness) (Figure 4). Increased visibility of vessels on SWI was categorized as absent (0) in 3/19 (scan delay range: 17.10 to 22.37 hours), discrete (1) in 9/19 (scan delay range: 3.52 to 23.75 hours), moderate (2) in 5/19 (scan delay range: 2.07 to 18.40 hours), or marked (3) in 1/19 decedents (scan delay: 20.13 hours).

Spearman's rank correlation computations revealed significant negative correlations between scan delay and adjusted FLAIR TI (*rho*=-.67, p=0.0032) and sum of the three ADC values (*rho*=-.57, p=0.0128). Significant positive correlations were found with the sum of increased T1WI signal intensity scores (*rho*=.68, p=0.0015), T2WI fat suppression scores (*rho*=.76, p=0.0001) and DWI rim-like increased signal intensity score (*rho*=.61, p=0.0053). The correlation with SWI vessel visibility score (*rho*=-.42, p=.08) was not significant. All significant correlations survived Bonferroni correction (number of tests = 6), except for the sum of ADC values.

*Brain MRI findings reflecting antemortem changes*

Recent and long-standing MRI signal changes are summarized in Table e-3 available from Dryad: https://doi.org/10.5061/dryad.4qrfj6q7p.

Figure 5 illustrates recent structural cerebral abnormalities in COVID-19 non-survivors.

Parenchymal brain MRI abnormalities were found in four decedents.

D2 presented subcortical macro- and micro-hemorrhages with posterior predominance, both supra- and infra-tentorially, which were best documented on SWI. The associated increased T1WI signal intensity in the larger lesions and overlying cortical edema

was suggestive of subacute hemorrhages (Figures 5 and 6). A previous brain MRI, obtained in November 2016, did not show any hemorrhage. This decedent died at the ICU.

D4 exhibited two small arciform subcortical hemorrhages, one right temporal and one right occipital on SWI, corresponding to a discrete linear signal loss on T1- and T2WI (Figures 5 and 6). There was no surrounding vasogenic edema, microbleeds or superficial hemosiderosis. White matter changes evocative of microvascular disease were limited, consisting in smooth periventricular hyperintensities, including caps around the ventricular horns and periventricular halos (Fazekas grade 1, Figure 6). No antemortem MRI was available for this patient. D4 died 24 hours after admission and had 115/86 mmHg of systolic/diastolic blood pressure at admission.

D7 showed superior precentral and parietal cortico-subcortical swelling associated with marked supratentorial white matter changes. Decedent's blood pressure measured 1-3 times/day in a COVID-19 ward oscillated between 90/55 and 140/80 mmHg during the five days before death.

D9 had extensive T2WI hazy hyperintensity in bilateral centrum semiovale and was hospitalized at ICU.

Four decedents had asymmetric olfactory bulbs with ipsilateral (D8) or without (D5, D11, D12) olfactory cleft obliteration. No other abnormality was found along the olfactory tract.

No signal abnormality was found in the brainstem, except in D10 who had a midline pontine signal abnormality evocative of capillary telangiectasia (Figure e-1 available from Dryad: https://doi.org/10.5061/dryad.4qrfj6q7p).

## Discussion

In this case series of COVID-19 non-survivors, we performed a systematic and comprehensive assessment of the abnormalities encountered on their early postmortem brain MRI. Changes related to postmortem signal changes were first analysed.[21–24] Then, antemortem changes were distinguished between presumed recent or chronic brain pathology, using common radiological markers and scales.[26–29]

The present population of COVID-19 non-survivors was typical of those previously reported in the literature,[31–33] in particular regarding age, comorbidities and complications leading to poor clinical outcome.

*Brain MRI findings reflecting postmortem changes*

Five brain MRI findings were attributed to postmortem changes. The significant correlation between quantitative evaluation of these changes and the scan delay reinforced this hypothesis. These findings were (i) the necessary adaptation of the FLAIR TI to obtain adequate water suppression, (ii) increased T1WI signal intensity of the deep nuclei, (iii) T2WI fat suppression, (iv) DWI rim-like increased signal intensity, and (v) decreased parenchymal ADC values. Overall, we attribute those observations, at least partly, to the low temperature of decedents' body (algor mortis) compared to that in vivo, greatly influencing T1, and to a lesser extent, T2 relaxation times.[34,35] These temperature changes were the common hypothesis formulated in existing postmortem literature,[21–24] of which we reproduce the above mentioned brain findings.

One observation, i.e., the increased SWI vessel visibility, was not investigated in previous postmortem brain MRI reports and did not significantly correlate with scan delay. While it could still represent a postmortem change, the lack of correlation could be explained by the multiplicity of factors, which may lead to such a phenomenon, e.g., decrease in

intravascular oxy/deoxyhemoglobin ratio, blood stagnation, decrease in brain temperature and possible premortem intravascular clotting associated with the putative endothelial injury caused by SARS-CoV-2.[36] It was however not present in the decedents with the most marked recent hemorrhagic (D2) or white matter (D9) changes and only discretely present in the decedent with cortical edema (D7, grade 1). It therefore warrants further investigation.

The main limitation of the present postmortem MRI virtopsy lies in the severe SARS-CoV-2 pathology characterizing all decedents, which may limit the generalization of observed postmortem brain MRI findings to other clinical settings.

*Brain MRI findings reflecting antemortem changes*

Parenchymal brain MRI abnormalities were observed in 4/19 decedents (21%), while asymmetric olfactory bulbs were found in 4 others (21%).

D2 had diffuse subcortical micro- and macro-bleeds with posterior predominance. Considering his clinico-biological context, these abnormalities were evocative of multifocal hemorrhagic lesions triggered by disseminated intravascular coagulation (DIC).[3738] DIC is indeed frequently observed in patients with severe COVID-19.[37] Nevertheless, intracerebral hemorrhage is also a possible and rather frequent (5-10% of patients) complication of ECMO, though diffuse micro-bleeds are only seen sporadically and do not display a posterior predominance.[39] A combination of different causes underlying intracranial hemorrhages in D2 has therefore to be considered, with blood-brain barrier breakdown possibly favored by SARS-CoV-2-related endothelial dysfunction as hypothetical synergic pathophysiological mechanism.

In D4, we observed two posterior macro-subcortical bleeds, which shared some similarities with those observed in D2. Their origin is arguably more difficult to interpret in the absence of previous brain MRI. Still, we suspect that pathophysiological mechanisms

other than the classical small vessel disease (SVD) and cerebral amyloid angiopathy (CAA) took place. SVD is associated with microbleeds and lacunes (posterior fossa, basal ganglia, supratentorial white matter), white matter hyperintensities and cortical infarcts.[40,41] Hemorrhages due to CAA are associated with large lobar macro-hemorrhage, lobar microbleeds,[25] cortical superficial siderosis,[42] white matter hyperintensities and enlargement of perivascular spaces in the centrum semiovale.[43] D4 instead presented an isolated left thalamic lacune and very mild white matter hyperintensities (Fazekas grade 1) for his age (79 years), no enlargement of perivascular spaces and no other hemorrhage. Although according to the modified Boston criteria,[25] the diagnosis of CAA is deemed "probable" in the presence of two lobar bleeds, it is so in the absence of other causes of hemorrhage. Other possible causes could be head trauma (not reported and unlikely given the imaging appearance of the bleeds), hypertension (normal blood pressure at admission with death after 24 hours, intracranial hemorrhage more often located in deep brain structures and associated with radiologic signs of SVD[44]), anticoagulant therapy (prophylactic anticoagulation in this decedent) or blood clots (D-dimers level not available). Considering the COVID-19 status of the decedent, it might be hypothesized that these two subcortical hemorrhages have been triggered by similar blood-brain barrier breakdown phenomena as in D2.

D7 showed superior precentral and parietal cortico-subcortical swelling associated with marked supratentorial white matter changes. These findings are evocative of posterior reversible encephalopathy syndrome (PRES). PRES refers to reversible vasogenic brain oedema predominating in posterior brain regions, which occurs in association with a variety of systemic disorders.[45,46] PRES is typically caused by endothelial injury related to abrupt blood pressure changes or direct effects of cytokines on the endothelium.[45,46] In D7, blood pressure monitored during her stay in a COVID-19 ward did not support the hypothesis that hypertension was at the origin of PRES in her case. PRES has been reported in patients with

normal blood pressure or hypotension.[45,46] In those patients, endothelial dysfunction from, e.g., the cytotoxic effects of infection (e.g., cytokine storm) is one of the considered pathophysiological mechanisms.[45,46] PRES has been reported in a young adult with COVID-19 who developed acute confusional state and transient cortical blindness.[47] PRES should therefore be considered as a potential complication of COVID-19.

D9 had extensive hazy T2WI hyperintensity of the centrum semiovale, of uncertain significance. This could be the manifestation of early edematous changes due to blood-brain barrier breakdown associated with hypoxia or deep watershed infarction. Still, unspecific chronic changes related to the decedent's metabolic disorders (hyperthyroidism and hyperaldosteronism) cannot be excluded. Interestingly, such hazy white matter T2WI hyperintensity has been reported in 37% of COVID-19 patients with neurological symptoms admitted to the ICU, for which a definite diagnosis was difficult to settle.[48]

In those 4 decedents with parenchymal brain MRI abnormalities, blood-brain barrier breakdown might be the common denominator between DIC-related lesions, PRES and centrum semiovale changes.[49] It might be caused by endothelial dysfunction related to severe COVID-19 (i.e., severe hypoxia, CID, cytokine storm) with or without direct SARS-CoV-2 infection of endothelial cells. Given the widespread endothelial expression of ACE2,[36] such hypothetical endothelial infection might lead to secondary intracerebral endothelial inflammation and activation. Both cytokine storm and SARS-CoV-2 infection of endothelial cells occur in severe COVID-19 leading to a widespread "endotheliitis".[36] Of note, we did not find in our series larger ischemic[13] or hemorrhagic[12] strokes that have been previously reported in COVID-19. This absence of large ischemic stroke may result from the widespread use of prophylactic or therapeutic anticoagulation in all decedents. This study therefore enlarges the clinical spectrum of possible vascular changes that can be found in patients with severe COVID-19.

Asymmetric olfactory bulbs with or without olfactory cleft obliteration were observed in 4/19 decedents. This may represent an MRI-correlate of anosmia frequently observed in SARS-CoV-2 patients and may support the neural retrograde hypothesis for SARS-CoV-2 CNS dissemination. Still, anosmia was not reported in any of the decedent — but it was not systematically assessed— and this study did not find any MRI signal abnormality downstream the olfactory tract. Normal olfactory bulb and tract with no sign of nasal congestion have been reported in one SARS-CoV-2 infected patient with acute anosmia.[8] Further studies are warranted to better understand the pathophysiological mechanisms of anosmia in COVID-19.

This study failed to find specific brainstem abnormalities, bringing no support to a brain-related contribution to respiratory distress in COVID-19.[6] Still, this does not exclude the possibility of SARS-CoV-2-related dysregulation of brainstem respiratory nuclei not observable on brain MRI.

*Limitations of the study*

First, due to our strict inclusion criteria, 70% of COVID-19 patients who died during the inclusion period at our institution were not included in the present study. Due to this high-level of decedents' exclusion, the study may not provide a complete picture of COVID-19-related brain MRI abnormalities. In particular, we only included decedents with positive detection of SARS-CoV-2 on nasopharyngeal swab specimen and a chest computed tomography (CT) scan typical of COVID-19 in order to reinforce the possible associations between postmortem brain MRI findings and COVID-19, or its complications. Due to this stringent inclusion criterion, the study does not investigate the possible occurrence of brain lesions in SARS-CoV-2 infected decedents without pulmonary involvement (see, e.g., [50]). We limited the delay between death and postmortem MRI data acquisition to <24h. This was

decided to reduce the effects of postmortem brain changes that could complicate the interpretation of brain MRI data.[21,22] The strong correlations found between the delay and the evolution of brain MRI signal do support this approach. We decided to exclude decedents with known focal brain lesions as this could complicate the interpretation of postmortem brain MRI data. Previously lesioned brain tissue may indeed represent an easier entryway for the virus to the brain due to, e.g., blood brain barrier breakdown. This might complicate the interpretation of the recent vs. long-lasting origin of antemortem brain MRI abnormalities.

Second, several limitations are intrinsic to the virtopsy approach used in this study. Interpretations of brain MRI findings are indeed complicated by (i) postmortem brain changes (see above), (ii) the global reduction of ADC that limits the use of this information for DWI data interpretation, and (iii) the lack of circulation preventing the use of both exogenous (gadolonium) and endogenous (e.g., blood oxygen level dependent signal, arterial spin labeling, time-of-flight angiography) tracers.[21,22] These intrinsic limitations forced us to adopt a systematic and descriptive approach to report the brain MRI findings and to provide prudent interpretation of those attributed to COVID-19, after reaching a multidisciplinary consensus.

Third, the design of this study was prospective in the sense that consecutive decedents fulfilling inclusion criteria during the inclusion period were all included in a prospective manner. The inclusion process therefore started at the time of death. This implied that, during the hospitalization, patients' clinical status was not systematically investigated in light of the objectives of the study. We relied on the medical records to get information about decedents' neurological status. With the high pressure of the COVID-19 outbreak on medical facilities and staff, stress was put on patients' respiratory and systemic status. Thus, the neurological status was not reported with full details in the critically ill or end-of-life patients such as the included decedents.

Finally, as this study did focus on COVID-19 non-survivors, it did not evaluate patients with COVID-19 and acute neurological symptoms (e.g., stroke, seizures, etc.) who survived. This study therefore provides an incomplete picture of COVID-19-related brain disorders, such as those previously reported and not found in this case series.[11,12,14] Still, this study provides novel insights into the possible types of brain lesions that can be observed in COVID-19.

**Acknowledgments**

The authors would like to express their most sincere gratitude to all the personnel of the morgue and of the PET-MR Unit of the CUB Hôpital Erasme. Their fantastic work and efforts made this study possible.

**Appendix 1. Authors**

| Name | Location | Contribution |
|---|---|---|
| Tim Coolen, MD | Department of Radiology, CUB Hôpital Erasme, Université libre de Bruxelles (ULB), Brussels, Belgium; Laboratoire de Cartographie fonctionnelle du Cerveau, UNI — ULB Neuroscience Institute, Université libre de Bruxelles (ULB), Brussels, Belgium | Study concept and design; data acquisition and analysis; interpretation of data; full access to all of the data in the study; responsible for the integrity of the data and the accuracy of the data analysis; statistical analyses; drafting the manuscript; critical revision of the manuscript for important intellectual content; shares first authorship with equal contributions. |
| Valentina Lolli, MD | Department of Radiology, CUB Hôpital Erasme, Université libre de Bruxelles (ULB), Brussels, Belgium; Laboratoire de Cartographie fonctionnelle du Cerveau, UNI — ULB Neuroscience Institute, Université libre de Bruxelles (ULB), Brussels, Belgium | Study concept and design; data acquisition and analysis; interpretation of data; full access to all of the data in the study; responsible for the integrity of the data and the accuracy of the data analysis; drafting the manuscript; critical revision of the manuscript for important intellectual content ; shares first authorship with equal contributions. |
| Niloufar Sadeghi, MD, PhD | Department of Radiology, CUB Hôpital Erasme, Université libre de Bruxelles (ULB), Brussels, Belgium | Study concept and design; data acquisition and analysis; interpretation of data; full access to all of the data in the study; responsible for the integrity of the data and the accuracy of the data analysis; drafting the manuscript; critical revision of the manuscript for important intellectual content. |
| Antonin Rovaï, PhD | Laboratoire de Cartographie fonctionnelle du Cerveau, UNI — ULB Neuroscience Institute, Université libre de Bruxelles (ULB), Brussels, Belgium; Department of Nuclear Medicine, CUB Hôpital Erasme, Université libre de Bruxelles (ULB), Brussels, Belgium | Interpretation of data; critical revision of the manuscript for important intellectual content |
| Nicola Trotta, PhD | Laboratoire de Cartographie fonctionnelle du Cerveau, UNI — ULB Neuroscience Institute, Université libre de Bruxelles (ULB), Brussels, Belgium; Department of Nuclear Medicine, CUB Hôpital Erasme, | Interpretation of data; critical revision of the manuscript for important intellectual content |

| | | |
|---|---|---|
| | Université libre de Bruxelles (ULB), Brussels, Belgium | |
| Fabio Silvio Taccone, MD, PhD | Intensive Care Unit, CUB Hôpital Erasme, Université libre de Bruxelles (ULB), Brussels, Belgium | Interpretation of data; critical revision of the manuscript for important intellectual content |
| Jacques Creteur, MD, PhD | Intensive Care Unit, CUB Hôpital Erasme, Université libre de Bruxelles (ULB), Brussels, Belgium | Interpretation of data; critical revision of the manuscript for important intellectual content |
| Sophie Henrard, MD | Department of Internal Medicine, CUB Hôpital Erasme, Université libre de Bruxelles (ULB), Brussels, Belgium | Interpretation of data; critical revision of the manuscript for important intellectual content |
| Jean-Christophe Goffard, MD, PhD | Department of Internal Medicine, CUB Hôpital Erasme, Université libre de Bruxelles (ULB), Brussels, Belgium | Interpretation of data; critical revision of the manuscript for important intellectual content |
| Olivier De Witte, MD, PhD | Department of Neurosurgery, CUB Hôpital Erasme, Université libre de Bruxelles (ULB), Brussels, Belgium | Study concept and design; interpretation of data; critical revision of the manuscript for important intellectual content |
| Gilles Naeije, MD, PhD | Department of Nuclear Medicine, CUB Hôpital Erasme, Université libre de Bruxelles (ULB), Brussels, Belgium; Department of Neurology, CUB Hôpital Erasme, Université libre de Bruxelles (ULB), Brussels, Belgium. | Interpretation of data; drafting the manuscript; critical revision of the manuscript for important intellectual content |
| Serge Goldman, MD, PhD | Laboratoire de Cartographie fonctionnelle du Cerveau, UNI — ULB Neuroscience Institute, Université libre de Bruxelles (ULB), Brussels, Belgium; Department of Nuclear Medicine, CUB Hôpital Erasme, Université libre de Bruxelles (ULB), Brussels, Belgium | Study concept and design; data acquisition and analysis; interpretation of data; full access to all of the data in the study; responsible for the integrity of the data and the accuracy of the data analysis; drafting the manuscript; critical revision of the manuscript for important intellectual content; obtained funding |
| Xavier De Tiège, MD, PhD | Laboratoire de Cartographie fonctionnelle du Cerveau, UNI — ULB Neuroscience Institute, Université libre de Bruxelles (ULB), Brussels, Belgium; Department of Nuclear Medicine, CUB Hôpital Erasme, Université libre de Bruxelles (ULB), Brussels, Belgium | Study concept and design; data acquisition and analysis; interpretation of data; full access to all of the data in the study; responsible for the integrity of the data and the accuracy of the data analysis; drafting the manuscript; critical revision of the manuscript for important intellectual content; obtained funding |

**References**


1. Zhu N, Zhang D, Wang W, et al. A Novel Coronavirus from Patients with Pneumonia in China, 2019. N Engl J Med. 2020;382:727–733.

2. Zhou P, Yang X-L, Wang X-G, et al. A pneumonia outbreak associated with a new coronavirus of probable bat origin. Nature. 2020;579:270–273.

3. Walls AC, Park Y-J, Tortorici MA, Wall A, McGuire AT, Veesler D. Structure, Function, and Antigenicity of the SARS-CoV-2 Spike Glycoprotein. Cell [online serial]. Epub 2020 Mar 6. Accessed at: http://dx.doi.org/10.1016/j.cell.2020.02.058.

4. Xia H, Lazartigues E. Angiotensin-converting enzyme 2 in the brain: properties and future directions. J Neurochem. 2008;107:1482–1494.

5. De Felice FG, Tovar-Moll F, Moll J, Munoz DP, Ferreira ST. Severe Acute Respiratory Syndrome Coronavirus 2 (SARS-CoV-2) and the Central Nervous System. Trends Neurosci [online serial]. Epub 2020 Apr 21. Accessed at: http://dx.doi.org/10.1016/j.tins.2020.04.004.

6. Li Y-C, Bai W-Z, Hashikawa T. The neuroinvasive potential of SARS-CoV2 may play a role in the respiratory failure of COVID-19 patients. J Med Virol [online serial]. Epub 2020 Feb 27. Accessed at: http://dx.doi.org/10.1002/jmv.25728.

7. Spinato G, Fabbris C, Polesel J, et al. Alterations in Smell or Taste in Mildly Symptomatic Outpatients With SARS-CoV-2 Infection. JAMA [online serial]. Epub 2020 Apr 22. Accessed at: http://dx.doi.org/10.1001/jama.2020.6771.

8. Galougahi MK, Ghorbani J, Bakhshayeshkaram M, Naeini AS, Haseli S. Olfactory Bulb Magnetic Resonance Imaging in SARS-CoV-2-Induced Anosmia: The First Report [online]. Academic Radiology 2020. Accessed at: http://dx.doi.org/10.1016/j.acra.2020.04.002.

9. Huang YH, Hanna Huang Y, Jiang D, Huang JT. SARS-CoV-2 Detected in Cerebrospinal Fluid by PCR in a Case of COVID-19 Encephalitis [online]. Brain, Behavior, and Immunity 2020. Accessed at: http://dx.doi.org/10.1016/j.bbi.2020.05.012.

10. Ye M, Ren Y, Lv T. Encephalitis as a clinical manifestation of COVID-19 [online]. Brain, Behavior, and Immunity 2020. Accessed at: http://dx.doi.org/10.1016/j.bbi.2020.04.017.

11. Moriguchi T, Harii N, Goto J, et al. A first Case of Meningitis/Encephalitis associated with SARS-Coronavirus-2. Int J Infect Dis [online serial]. Epub 2020 Apr 3. Accessed at: http://dx.doi.org/10.1016/j.ijid.2020.03.062.

12. Sharifi-Razavi A, Karimi N, Rouhani N. COVID 19 and Intra cerebral hemorrhage: Causative or Coincidental [online]. New Microbes and New Infections 2020. p. 100669. Accessed at: http://dx.doi.org/10.1016/j.nmni.2020.100669.

13. Oxley TJ, Mocco J, Majidi S, et al. Large-Vessel Stroke as a Presenting Feature of Covid-19 in the Young [online]. New England Journal of Medicine 2020. p. e60. Accessed at: http://dx.doi.org/10.1056/nejmc2009787.

14. Poyiadji N, Shahin G, Noujaim D, Stone M, Patel S, Griffith B. COVID-19-associated Acute Hemorrhagic Necrotizing Encephalopathy: CT and MRI Features. Radiology. Epub 2020 Mar 31.:201187.

15. Mao L, Jin H, Wang M, et al. Neurologic Manifestations of Hospitalized Patients With Coronavirus Disease 2019 in Wuhan, China. JAMA Neurol [online serial]. Epub 2020 Apr 10. Accessed at: http://dx.doi.org/10.1001/jamaneurol.2020.1127.

16. Kellum JA, Lameire N, KDIGO AKI Guideline Work Group. Diagnosis, evaluation, and management of acute kidney injury: a KDIGO summary (Part 1). Crit Care. 2013;17:204.

17. Henrion J. Hypoxic hepatitis [online]. Liver International 2012. p. 1039–1052. Accessed at: http://dx.doi.org/10.1111/j.1478-3231.2011.02655.x.

18. Taylor F, Toh C-H, Hoots K, Wada H, Levi M. Towards Definition, Clinical and Laboratory Criteria, and a Scoring System for Disseminated Intravascular Coagulation [online]. Thrombosis and Haemostasis 2001. p. 1327–1330. Accessed at: http://dx.doi.org/10.1055/s-0037-1616068.

19. Shi S, Qin M, Shen B, et al. Association of Cardiac Injury With Mortality in Hospitalized Patients With COVID-19 in Wuhan, China. JAMA Cardiol [online serial]. Epub 2020 Mar 25. Accessed at: http://dx.doi.org/10.1001/jamacardio.2020.0950.

20. Tofts PS, Jackson JS, Tozer DJ, et al. Imaging cadavers: cold FLAIR and noninvasive brain thermometry using CSF diffusion. Magn Reson Med. 2008;59:190–195.

21. Offiah CE, Dean J. Post-mortem CT and MRI: appropriate post-mortem imaging appearances and changes related to cardiopulmonary resuscitation. Br J Radiol. 2016;89:20150851.

22. Grabherr S, Egger C, Vilarino R, Campana L, Jotterand M, Dedouit F. Modern post-mortem imaging: an update on recent developments. Forensic Sci Res. 2017;2:52–64.

23. Wagensveld IM, Blokker BM, Wielopolski PA, et al. Total-body CT and MR features of postmortem change in in-hospital deaths [online]. PLOS ONE 2017. p. e0185115. Accessed at: http://dx.doi.org/10.1371/journal.pone.0185115.

24. Kobayashi T, Shiotani S, Kaga K, et al. Characteristic signal intensity changes on postmortem magnetic resonance imaging of the brain. Jpn J Radiol. 2010;28:8–14.

25. Greenberg SM, Charidimou A. Diagnosis of Cerebral Amyloid Angiopathy: Evolution of the Boston Criteria. Stroke. 2018;49:491–497.

26. Fazekas F, Chawluk JB, Alavi A, Hurtig HI, Zimmerman RA. MR signal abnormalities at 1.5 T in Alzheimer's dementia and normal aging [online]. American Journal of Roentgenology 1987. p. 351–356. Accessed at: http://dx.doi.org/10.2214/ajr.149.2.351.

27. Maclullich AMJ, Wardlaw JM, Ferguson KJ, Starr JM, Seckl JR, Deary IJ. Enlarged perivascular spaces are associated with cognitive function in healthy elderly men. J Neurol Neurosurg Psychiatry. 2004;75:1519–1523.

28. Doubal FN, MacLullich AMJ, Ferguson KJ, Dennis MS, Wardlaw JM. Enlarged perivascular spaces on MRI are a feature of cerebral small vessel disease. Stroke. 2010;41:450–454.

29. Harper L, Barkhof F, Fox NC, Schott JM. Using visual rating to diagnose dementia: a critical evaluation of MRI atrophy scales. J Neurol Neurosurg Psychiatry. 2015;86:1225–1233.

30. Ng SES, Low AMS, Tang KK, Chan YH, Kwok RK. Value of quantitative MRI biomarkers (Evans' index, aqueductal flow rate, and apparent diffusion coefficient) in idiopathic normal pressure hydrocephalus. J Magn Reson Imaging. 2009;30:708–715.

31. Du R-H, Liang L-R, Yang C-Q, et al. Predictors of Mortality for Patients with COVID-19 Pneumonia Caused by SARS-CoV-2: A Prospective Cohort Study. Eur Respir J [online serial]. European Respiratory Society; Epub 2020 Jan 1. Accessed at: https://erj.ersjournals.com/content/early/2020/04/01/13993003.00524-2020.abstract. Accessed April 29, 2020.

32. Guan W-J, Liang W-H, He J-X, Zhong N-S. Cardiovascular comorbidity and its impact on patients with Covid-19 [online]. European Respiratory Journal 2020. p. 2001227. Accessed at: http://dx.doi.org/10.1183/13993003.01227-2020.

33. Zhou F, Yu T, Du R, et al. Clinical course and risk factors for mortality of adult inpatients with COVID-19 in Wuhan, China: a retrospective cohort study [online]. The Lancet 2020. p. 1054–1062. Accessed at: http://dx.doi.org/10.1016/s0140-6736(20)30566-3.

34. Nelson TR, Tung SM. Temperature dependence of proton relaxation times in vitro. Magn Reson Imaging. 1987;5:189–199.

35. Zech W-D, Schwendener N, Persson A, Warntjes MJ, Jackowski C. Temperature dependence of postmortem MR quantification for soft tissue discrimination. Eur Radiol. 2015;25:2381–2389.

36. Varga Z, Flammer AJ, Steiger P, et al. Endothelial cell infection and endotheliitis in COVID-19. Lancet [online serial]. Epub 2020 Apr 20. Accessed at: http://dx.doi.org/10.1016/S0140-6736(20)30937-5.

37. Lillicrap D. Disseminated intravascular coagulation in patients with 2019-nCoV pneumonia. J. Thromb. Haemost. 2020. p. 786–787.

38. Lucas A. Disseminated Intravascular Coagulation – The Hemorrhagic Hurricane and the Cytokine Storm [online]. Journal of Clinical & Experimental Cardiology 2013. Accessed at: http://dx.doi.org/10.4172/2155-9880.1000e127.

39. Luyt C-E, Bréchot N, Demondion P, et al. Brain injury during venovenous extracorporeal membrane oxygenation. Intensive Care Med. 2016;42:897–907.

40. Wardlaw JM, Smith C, Dichgans M. Small vessel disease: mechanisms and clinical implications. Lancet Neurol. 2019;18:684–696.

41. Staals J, Makin SDJ, Doubal FN, Dennis MS, Wardlaw JM. Stroke subtype, vascular risk factors, and total MRI brain small-vessel disease burden. Neurology. 2014;83:1228–1234.

42. Charidimou A, Jäger RH, Fox Z, et al. Prevalence and mechanisms of cortical superficial siderosis in cerebral amyloid angiopathy. Neurology. 2013;81:626–632.

43. Charidimou A, Boulouis G, Pasi M, et al. MRI-visible perivascular spaces in cerebral amyloid angiopathy and hypertensive arteriopathy. Neurology. 2017;88:1157–1164.

44. Caceres JA, Goldstein JN. Intracranial hemorrhage. Emerg Med Clin North Am. 2012;30:771–794.

45. Fugate JE, Rabinstein AA. Posterior reversible encephalopathy syndrome: clinical and radiological manifestations, pathophysiology, and outstanding questions. Lancet Neurol. 2015;14:914–925.

46. Hinduja A. Posterior Reversible Encephalopathy Syndrome: Clinical Features and Outcome. Front Neurol. 2020;11:71.

47. Kaya Y, Kara S, Akinci C, Kocaman AS. Transient cortical blindness in COVID-19 pneumonia; a PRES-like syndrome: Case report. J Neurol Sci. 2020;413:116858.

48. Kandemirli SG, Dogan L, Sarikaya ZT, et al. Brain MRI Findings in Patients in the Intensive Care Unit with COVID-19 Infection. Radiology. Epub 2020 May 8.:201697.

49. Stokum JA, Gerzanich V, Marc Simard J. Molecular pathophysiology of cerebral edema [online]. Journal of Cerebral Blood Flow & Metabolism 2016. p. 513–538. Accessed at: http://dx.doi.org/10.1177/0271678x15617172.

50. Inciardi RM, Lupi L, Zaccone G, et al. Cardiac Involvement in a Patient With Coronavirus Disease 2019 (COVID-19) [online]. JAMA Cardiology 2020. Accessed at: http://dx.doi.org/10.1001/jamacardio.2020.1096.

**Table 1. Decedents' Characteristics**

| | |
|---|---|
| **Age** | 77 y (range: 49 – 94 y) |
| **Gender** | 5 females, 14 males |
| **Comorbidities** | |
| Hypertension | 16/19 (84%) |
| Cardiac disease | 7/19 (37%) |
| Diabetes | 6/19 (32%) |
| Chronic obstructive pulmonary disease | 6/19 (32%) |
| Malignancy | 5/19 (26%) |
| Body mass index (mean, range) | 29, (range:18 – 42) \| 95% >25 |
| Smoking | 0/19 active<br>5/19 (26%) ex-smoker |
| Cognitive impairment | 4/19 (21%) |
| **Symptoms on admission** | |
| Fever (>38.5° C) | 5/19 (26%) |
| Cough | 10/19 (53%) |
| Dyspnea | 18/19 (95%) |
| Gastrointestinal symptoms | 4/19 (21%) |
| **Central nervous system symptoms on admission** | |
| Headache | 2/19 (10%) |
| Agitation, confusion, disorientation | 5/19 (26%) |
| Seizure | 1/19 (5%, 2 days before admission) |
| **Complications during hospital/ICU stay** | |
| Respiratory failure | 15/19 (79%) |
| Acute kidney injury | 14/19 (74%) |
| Acute cardiac injury | 18/19 (95%) |
| Septic shock / Multiple Organ Failure | 4/19 (21%) |

**Legend of the Figures**

**Figure 1:** Algor mortis-related T1-weighted imaging increased signal intensity of deep nuclei. Zoomed axial slices centered on the basal ganglia (A), substantia nigra and red nuclei (B) and dentate nuclei (C). In the first column (D11, scan delay of 3.38 hours), no clear high T1 signal (grade 0) is visible in the deep nuclei. In the second column (D7, scan delay of 5.05 hours), there is mildly (grade 1) increased T1 signal intensity in the substantia nigra and red nuclei. In the third column (D19, scan delay of 18.40 hours), more marked (grade 2) T1 high signal is seen in bilateral pallidi, postero-lateral thalami, substantia nigra as well as in red and dentate nuclei. Of note, there is focal signal decrease in the internal aspect of the pallidi in D7 consistent with mild, non-pathological mineralization. All images are displayed in radiological convention.

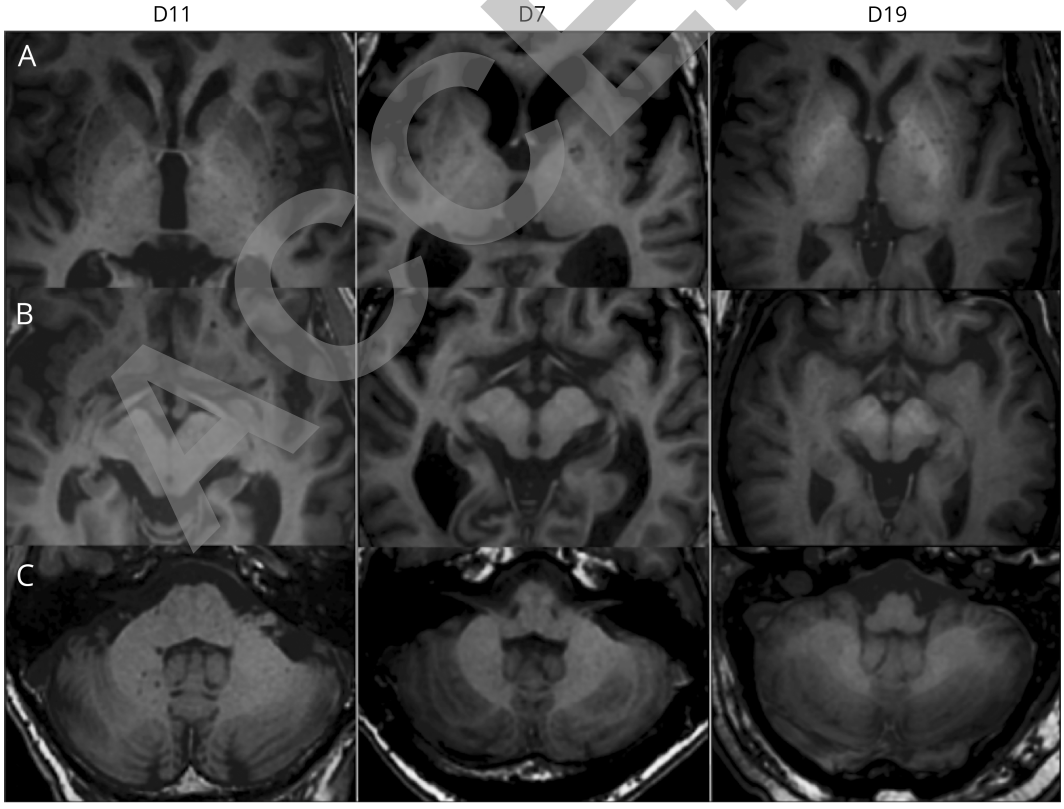

**Figure 2:** Algor mortis-related fat suppression on T2-weighted imaging. Axial images zoomed on the orbital region. (A) D4, scan delay of 2.07 hours: clear fat signal suppression in the right subcutaneous fat and very mildly decreased signal intensity of orbital fat. (B) D10, scan delay of 18.75 hours: clear suppression of both subcutaneous and orbital fat. All images are displayed in radiological convention.

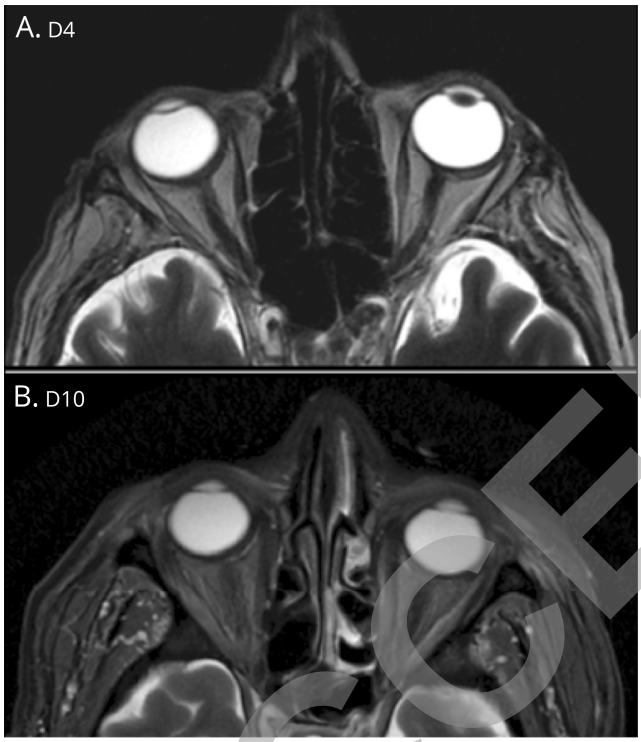

**Figure 3:** Cortical and periventricular rim of increased DWI signal intensity. Postmortem rim-like high signal of the cortical ribbon and ventricular wall on DWI was classified as incomplete (A, D4, scan delay of 2.07 hours) or complete (B, D15, scan delay of 16.77 hours). All images are displayed in radiological convention.

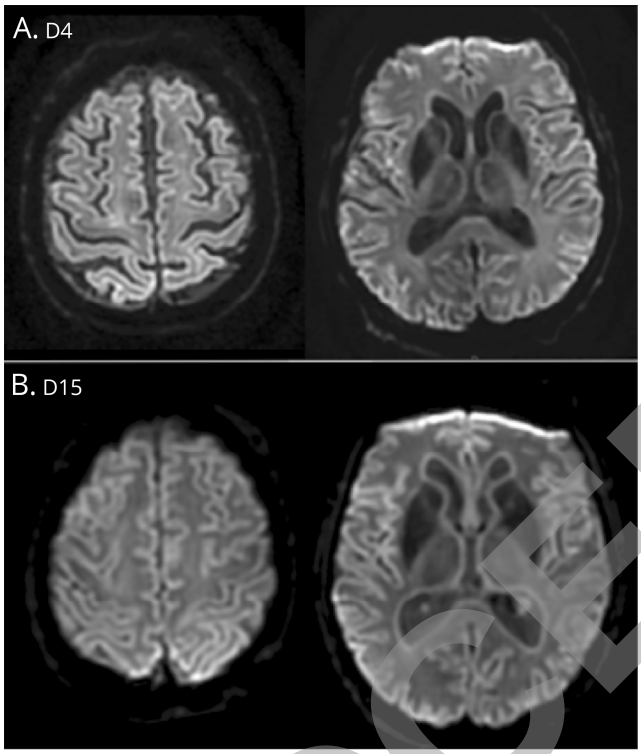

**Figure 4:** Postmortem increased vessel visibility on SWI sequence. The grading system developed in this study for vessel visibility is illustrated for each grade by supratentorial (A) and infratentorial (B) images on axial minimum intensity projections (10-mm thick). First column, no dilatation, grade 0 (D9, scan delay of 17.10 hours), apparent caliber of vessels on SWI is similar to that in vivo. Second column, discrete, grade 1 (D3, scan delay of 17.82 hours), slightly increased conspicuity of superficial vessels. Third column, moderate, grade 2 (D4, scan delay of 2.07 hours); fourth column, marked, grade 3 (D1, scan delay of 20.13 hours), visibility of superficial vessels is increased and deep perforating vessels become gradually apparent from grade 2 to 3. All images are displayed in radiological convention.

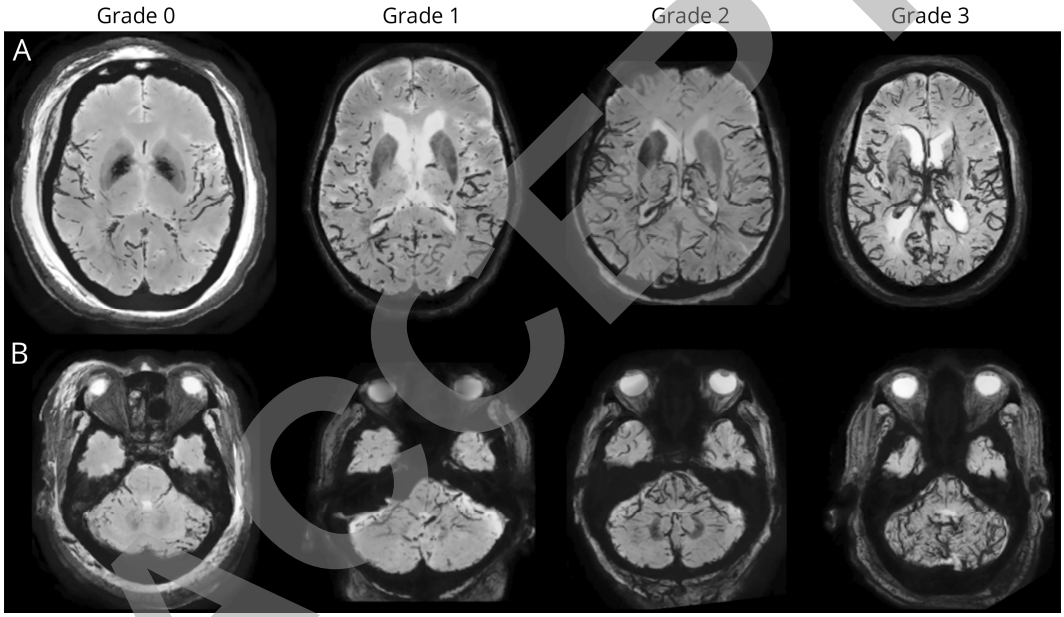

**Figure 5:** Postmortem brain MRI findings in five decedents (D2, D4, D7, D8, D9). For each decedent, two axial slices of their chest CT scan (first two images on the left) are provided to illustrate the typical SARS-CoV-2-related ground-glass multifocal lung opacities (delay between chest CT scan and death: 10 days, D2; 1 day D4; 7 days, D7; 21 days, D8; 2 days, D9). D2 (A) had diffuse micro- and macro-bleeds with parieto-occipito-temporal predominance, also involving the splenium of corpus callosum, left superior frontal sulcus and bilateral cerebellum, as demonstrated on the susceptibility weighted imaging (SWI) sequence. D4 (B) presented with two isolated arciform subcortical macro-bleeds in the right occipital and temporal lobes, also visible on the SWI sequence. D7 (C) displayed cortical and subcortical high FLAIR signal intensity and swelling in the bilateral superior precentral gyri and superior parietal lobules, while the posterior fossa was spared. D8 (D.a) had a relatively inflated left olfactory bulb associated with ipsilateral obliteration of the olfactory cleft. D9 (D.b) showed bilateral, extensive and hazy FLAIR high signal intensity of the bilateral centrum semiovale. All images are displayed in radiological convention.

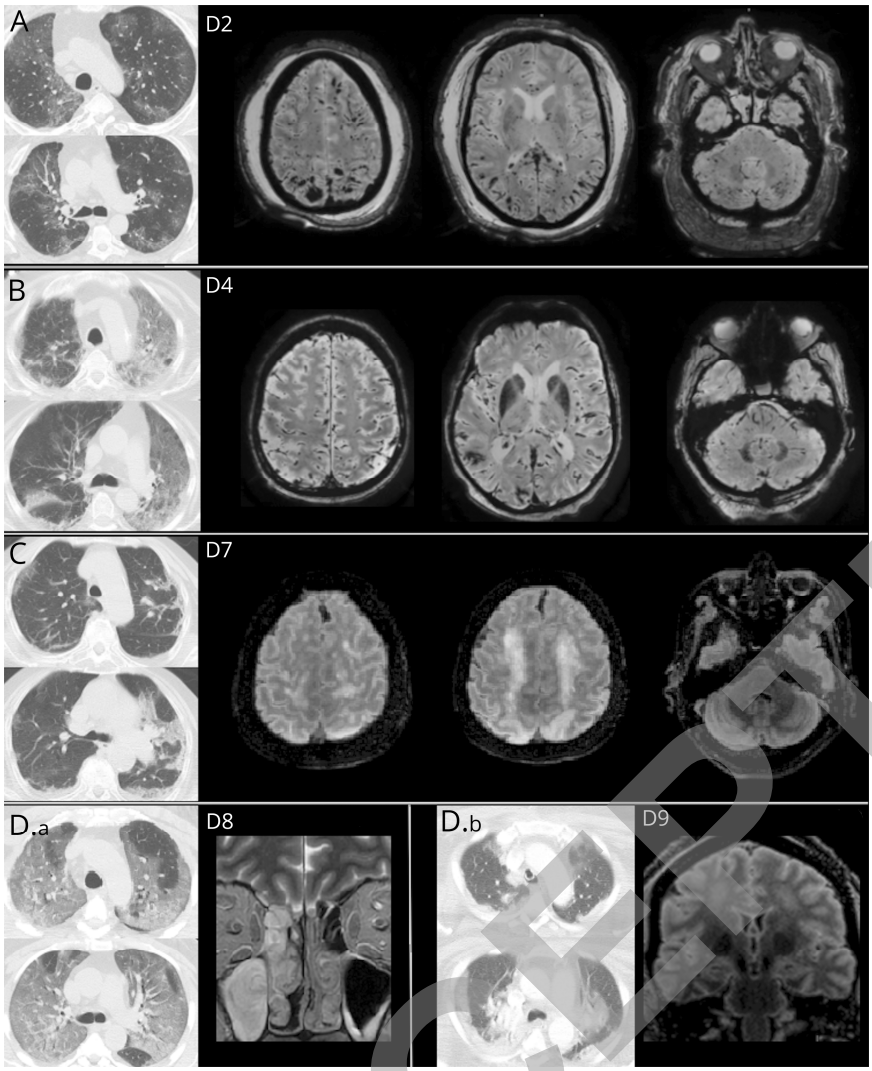

**Figure 6:** Additional illustrations for D2 (A) and D4 (B). Subcortical hemorrhagic lesions are depicted on the left in focused SWI and T1WI axial image pairs. The right parietal macro-hemorrhage of D2 presented a clear T1WI hyperintensity, while it is not the case for D4 and the smaller hemorrhagic lesions of D2. Reformatted axial FLAIR images on the right show mild cortical edema overlying another right parietal macro-hemorrhage in D2. D2 did not present white matter changes and D4 had only weak FLAIR signal changes in the periventricular white matter (Fazekas grade 1) with limited cortico-subcortical atrophy and no micro-bleed (one left thalamic lacune was observed). All images are displayed in radiological convention.